



## Technical note: Isotopic fractionation of evaporating waters: effect of sub-daily atmospheric variations and eventual depletion of heavy isotopes.

Francesc Gallart<sup>1</sup>, Sebastián González-Fuentes<sup>2</sup>, Pilar Llorens<sup>1</sup>

5 <sup>1</sup>Surface Hydrology and Erosion group, IDAEA, CSIC. Barcelona, 08034, Spain  
<sup>2</sup>Groundwater and Hydrogeochemistry group, IDAEA, CSIC. Barcelona, 08034, Spain

Correspondence to: Francesc Gallart (francesc.gallart@idaea.csic.es)

**Abstract.** Isotopic fractionation of evaporating waters has been studied constantly in recent decades, particularly because it enables calculation of both the volume of water evaporated from a water body and the isotopic composition of its source water. We studied the stable water isotope of an artificial pan filled with water in a sub-humid environment, in order to put into practice an operational method for estimating the time since disconnection of riverine pools when these are sampled for the quality of aquatic life.

Results indicate that: (i) when about 70% of pan water had evaporated and its isotope became enriched in heavy isotopes, some subsequent periods of depletion instead of enrichment happened, and (ii) the customary application of isotopic fractionation equations to determine the isotopic composition of the water in the pan using weekly averaged atmospheric conditions (temperature and relative humidity) strongly underestimated the changes observed, but predicted an early depletion of heavy isotopes. The first result, rarely reported in the literature, was found to be fully consistent with the early studies of the isotope of evaporating waters. The second one could be attributed to that weekly averages of temperature and relative humidity strongly overestimated air relative humidity during daylight periods of active evaporation. However, when the fractionation equations were parameterized using temperature and relative humidity weighted by potential evapotranspiration at sub-hourly time steps, they adequately reproduced the observed isotopic composition of the water in the pan, including the late periods of heavy isotope depletion. Our results should be taken into account when fractionation equations are applied in areas with relatively humid climates.

### 1 Introduction

25 There is increasing interest in the use of stable isotopes in open, soil and xylem waters to study either the volume of evaporated water or the original composition of the source water. The following articles synthesized published studies of open water (Skrzypek *et al.*, 2015), of soil and vegetation (Benettin *et al.*, 2019) and of rainfall interception processes (Allen *et al.*, 2017). In these studies, atmospheric parameters used in fractionation equations were averaged for weekly or monthly periods.

30 During evaporation of water in a natural environment, lighter water molecules usually vaporize faster than heavier ones, so that the remaining water body becomes enriched in heavier isotopes (Craig *et al.*, 1963). However, heavy isotope concentrations in water evaporating into open air increase asymptotically to a stationary isotopic state, as the mass of water in the water body decreases to zero. This effect is attributed to a rapid molecular exchange of isotopes between the water body and the atmospheric vapour, which predominates over the net isotopic effect of a simple evaporation process (Craig *et al.*, 1963). This isotopic exchange in either direction between liquid or vapour water has been identified, for example, in canopy interception processes, when air humidity is near to saturation (Allen *et al.*, 2017).

Gonfiantini (1986) showed that stationary isotopic concentrations ( $\delta^*$ ) depend mainly on air relative humidity to the extent that, when air relative humidity is low,  $\delta^*$  concentrations are practically unreachable; whereas, when it approaches 95%,



these can be reached when only about 20% of water had evaporated. For example, Fontes and Gonfiantini (1967) observed  
40 the depletion of heavy isotopes in the late desiccation stages of the Saharan Sebkh el Melah lake.

Most temporary rivers, from the cessation of flow to the total desiccation of the river bed, undergo a disconnected pools  
phase (Gallart *et al.*, 2017). As the aquatic life in these pools naturally changes after the flow cessation (Bonada *et al.*, 2020),  
the time between disconnection of these pools and sampling is information needed for assessing their biological quality. To  
implement an operational procedure to estimate the time since disconnection of river pools, based on the study of water  
45 stable isotopes, an artificial pan was set up in a location with a sub-humid climate, as a counterweight to the more frequent  
studies in dry climates.

The purpose of this technical note is to describe and analyse the observation of late periods of heavy isotope depletion  
instead of enrichment in the artificial pan, and the inaccuracy of the results when isotopic fractionation equations use time-  
averaged atmospheric conditions.

## 50 2 Data and Methods.

The experiment was performed in the Vallcebre Research Catchments (Eastern Pyrenees, Iberian Peninsula). Climate is sub-  
humid Mediterranean; mean temperature is 9.1°C, mean annual precipitation is 880 mm and mean annual potential  
evapotranspiration is 818 mm (Llorens *et al.*, 2018).

A round steel pan (Figure 1) was filled with 70 L of water from a nearby spring, partly buried in the ground and protected  
55 against precipitation by a lid of clear methacrylate installed 0.5 m above the pan's surface, to allow air circulation. A net  
stopped animals drinking. Bulk rainfall was sampled with a 180-mm diameter funnel connected to a 1-L plastic bottle with a  
pipe with a loop to prevent evaporation.

Bulk rainfall and water in the pan were sampled weekly from June to October 2020, when the pan had practically dried out  
(19 weeks).

60 Air temperature (T) and relative humidity (RH) (Vaisala, Finland), net radiation (Kipp and Zonen, The Netherlands) and  
wind speed (Thies Clima, Germany) were measured every 10 s and recorded at 5-min intervals by a data logger (Data Taker,  
Australia) in a meteorological station adjacent to the sampled pan.

Water samples were analysed for their stable isotope ratios ( $^{18}\text{O}$  and  $^2\text{H}$ ) via cavity ring-down spectroscopy (Picarro L2120-i,  
Picarro Inc., USA) at the laboratory of the Centre of Hydrogeology, University of Málaga. The precision of the isotope ratio  
65 measurements was reported as  $< 0.1\%$  for  $\delta^{18}\text{O}$  and  $< 0.4\%$  for  $\delta^2\text{H}$ . The data were expressed in the  $\delta$ -notation as parts per  
mil (‰) relative to Vienna Standard Mean Ocean Water.

The isotopic composition ( $\delta_L$ , ‰) of the residual water in the pan was calculated weekly for  $^{18}\text{O}$  and  $^2\text{H}$ , as in Gonfiantini  
(1986):

$$\delta_L = (\delta_0 - \delta^*)(1 - x)^m + \delta^* \quad (1)$$

70 where  $\delta_0$  is the initial isotopic composition,  $\delta^*$  the stationary isotopic composition reached when the remaining water in a  
pool tends to 0,  $m$  is the slope of the temporal enrichment (Gibson *et al.*, 2016), and  $x$  is the fraction of water volume that  
evaporated. Thus,  $1-x$  is the residual volume fraction.

The coefficients of equation 1 were calculated as follows:

$$\delta^* = \frac{(h\delta_A + \varepsilon_k + \varepsilon^+ / \alpha^+)}{(h - 10^{-3} \cdot (\varepsilon_k + \varepsilon^+ / \alpha^+))} \quad (2)$$

$$75 \quad m = \frac{(h - 10^{-3} \cdot (\varepsilon_k + \varepsilon^+ / \alpha^+))}{(1 - h + 10^{-3} \cdot \varepsilon_k)} \quad (3)$$



Where  $h$  (-) is the relative humidity,  $\delta_A$  (‰) is the isotopic composition of the atmospheric moisture,  $\epsilon_k$  (‰) the kinetic fractionation factor,  $\epsilon^+$  (‰) the isotopic separation between liquid and vapour and  $\alpha^+$  (‰) the equilibrium fractionation factor.

$\delta_A$  was assumed to be in equilibrium with the isotopic composition of precipitation  $\delta_P$  and was calculated as in Gibson *et al.* (2008):

$$\delta_A = (\delta_P - \epsilon^+)/\alpha^+ \quad (4)$$

$\epsilon_k$  was calculated as in Gat (1996) and Horita *et al.* (2008):

$$\epsilon_k = \theta n(1 - h)(1 - D_i/D)10^3 \quad (5)$$

Where  $\theta$  is a weighting term that can be assumed equal to 1 for a small body of water whose evaporation flux does not perturb the ambient moisture significantly (Gat, 1996). The factor  $n$ , which accounts for the aerodynamic regime above the evaporating liquid–vapour interface, was assumed to be 0.5 (turbulent) as for an open water body.  $D_i/D$  is the diffusivity ratio between light and heavy isotopes. Following (Merlivat, 1978)  $D_i/D$  is 0.9755 and 0.9723 for  $^2\text{H}$  and  $^{18}\text{O}$ , respectively.

$\epsilon^+$  was obtained from:

$$\epsilon^+ = (\alpha^+ - 1)10^3 \quad (6)$$

where  $\alpha^+$  is calculated from the absolute temperature  $T$  (°K), as in Horita & Wesolowski (1994):

$$10^3 \ln(\alpha^+) = 1158.8 \left( T^3 / 10^9 \right) - 1620.1 \left( T^2 / 10^6 \right) + 794.84 \left( T / 10^3 \right) - 161.04 + 2.9992 \left( 10^9 / T^3 \right) \quad (7)$$

for  $^2\text{H}$ , and

$$10^3 \ln(\alpha^+) = -7.685 + 6.7123 \left( 10^3 / T \right) - 1.6664 \left( 10^6 / T^2 \right) + 0.3504 \left( 10^9 / T^3 \right) \quad (8)$$

for  $^{18}\text{O}$ .

95

In a second step, to obtain daily and weekly  $T$  and  $\text{RH}$  values weighted with the evaporative flux, we calculated sub-hourly water evaporation rates in the pan using the Penman-Monteith equation parameterized as for reference evapotranspiration (Allen *et al.*, 1998).

### 3 Results and Discussion.

100 Figure 2a shows the time series of the isotopic composition ( $\delta^{18}\text{O}$ ) of the water sampled in the pan. During the first weeks the water became rapidly enriched, but became depleted after about two and a half months (71 days), when the relative volume of water in the pan was below 20%. Figure 2b shows that all the samples were located close to the same Local Evaporation Line (LEL), regardless of whether the water became enriched or depleted.

Our observations are fully consistent with the rationale that the stationary concentration ( $\delta^*$ ) drives the changes in the pan water (Craig *et al.*, 1963; Gonfiantini, 1987). Indeed, if we apply equation (1) to our pan water volume changes, we find that the isotopic composition of the residual water ( $\delta_L$ ) approaches  $\delta^*$  for both enriched and depleted trends of water samples. Once heavy isotope concentrations close to the stationary ones were reached in the pan, temporal changes in the atmospheric conditions, particularly the increase in air  $\text{RH}$ , as shown in Figure 3, might cause the decrease of  $\delta^*$ . In this case, the water in the pan would become depleted in heavy isotopes, showing that “molecular exchange with atmospheric water vapour predominates over the net isotopic effect of a simple evaporation process” (Craig *et al.*, 1963). Mass balance calculations showed that light isotopes declined throughout the experiment, demonstrating that evaporation rates always exceeded condensation ones (Figure A1 in Appendix A).

However, when equation (1) was used to calculate the isotopic composition of the water in the pan using weekly averages of  $T$  and  $\text{RH}$ , the results correctly simulated the isotopic composition of the water in the pan when relative volume of water in the pan was still higher than 60%, but largely underestimated the observed concentrations when the relative volume was

115



smaller. Figures 4a (chronicle of  $\delta^{18}\text{O}$ ) and 4b (dual plot) show the underestimation of the observed concentrations by equation (1) due to the marked diminution of the  $\delta^*$  values.

Given the high dependence of these stationary concentrations on RH (Gofiantini, 1987), an incorrect assessment of the effective value of RH was deemed the most likely cause of the underestimation of the measured isotopic composition using equation (1).

Figure 5 shows the 5-minute variations of RH and potential evaporation on September 4, a late-summer day selected to demonstrate the effect of the weighting of RH on  $\delta^*$  values. For this day, average daily RH was 74%, whereas when RH was weighted with potential evaporation the mean value was 52%. With equation (2) these RH values correspond to  $\delta^{*18}\text{O}$  concentrations of 5.94 and 22.15 ‰, respectively. Figures A2 and A3 show, for all the sampling dates, the differences in the daily values of T and RH when obtained by either time-averaging or evaporation flux-weighting and the corresponding differences in the estimates of  $\delta^*$  concentrations.

Subsequently, following the recommendation made by some authors (e.g. Allison and Leaney, 1982; Gibson, 2002; Gibson *et al.*, 2008), we used T and RH weighted with potential evaporation for parameterizing equation (1).

Figure 6a (chronicle of  $\delta^{18}\text{O}$ ) and 6b (dual plot) show the series of  $\delta^{18}\text{O}$  observed and simulated and  $\delta^*$  for the studied period. The results clearly improved when equation (1) was applied with T and RH weighted for potential evaporation, to the point of adequate simulation. Mean absolute errors decreased by a quotient of 4, from 19.31 and 3.78‰ for  $\delta^2\text{H}$  and  $\delta^{18}\text{O}$ , respectively, to 4.88 and 0.87‰. Figure A4 compares simulated *versus* observed concentrations for both isotopes and parameterisations.

#### 4 Final Remarks.

Our observations help to recall that isotopic fractionation by evaporation in a natural environment is not a simple distillation process but an exchange between liquid water and atmospheric water vapour. This is particularly relevant when air humidity is high and the evaporating water is already enriched in heavy isotopes.

Waters suffering prolonged evaporation tend to stationary heavy isotope concentrations ( $\delta^*$ ) that approach rainfall isotopic content when air humidity is near to saturation. In drier conditions, these  $\delta^*$  rapidly increase with decreasing air humidity and become detached from precipitation and atmospheric moisture isotopic content.

When the isotopic content of evaporating waters is used to calculate the volume of water evaporated, the susceptibility of heavy isotope depletion periods should be taken into account. Fortunately, when the target is to calculate the isotopic content of the source waters, these depletion periods follow the same LEL slope as enrichment periods.

The appropriateness of using temperature and relative humidity weighted by the evaporation flux for fractionation studies has been underlined by several authors (e.g. Allison and Leaney, 1982; Gibson, 2002; Gibson *et al.*, 2008; 2016). However, in practice this recommendation is not usually followed (except, for example, Mayr *et al.*, 2007), particularly where air humidity is low (e.g. Hamilton *et al.*, 2005; Skrzypek *et al.*, 2015) or when monthly or seasonal periods are investigated (e.g. Benettin *et al.*, 2018).

#### References

- Allen, R. G., Pereira, L. S., Raes, D., and Smith, M.: Crop evapotranspiration-Guidelines for computing crop water requirements. FAO Irrigation and drainage paper 56. FAO, Rome, 300(9), D05109, WAT 006, <https://www.fao.org/3/x0490e/x0490e00.htm>, 1998.
- Allen, S. T., Keim, R. F., Barnard, H. R., McDonnell, J. J., and Brooks, J. R.: The role of stable isotopes in understanding rainfall interception processes: a review, WIREs Water 2017, 4:e1187, doi: 10.1002/wat2.1187, 2017



- 155 Allison, G.B. and Leaney, F.W.: Estimation of isotopic exchange parameters using constant-feed pans, *J. Hydrol.* 55, 151–161, doi: 10.1002/wat2.1187, 1982.
- Benettin, P., Volkman, T. H., von Freyberg, J., Frentress, J., Penna, D., Dawson, T. E., and Kirchner, J. W.: Effects of climatic seasonality on the isotopic composition of evaporating soil waters, *Hydrol. Earth Syst. Sc.*, 22(5), 2881–2890, doi:10.5194/hess-22-2881-2018, 2018.
- 160 Bonada, N., Cañedo-Argüelles, M., Gallart, F., von Schiller, D., Fortuño, P., Latron, J., Llorens, P., Múrria, C., Soria, M. and Vinyoles, D.: Conservation and Management of Isolated Pools in Temporary Rivers, *Water*, 2020, 12, 2870, doi:10.3390/w12102870, 2020.
- Craig, H., Gordon, L. I., and Horibe, Y.: Isotopic exchange effects in the evaporation of water: 1. Low-temperature experimental results. *J. Geophys. Res.*, 68(17), 5079–5087. Doi: 10.1029/JZ068i017p05079, 1963.
- 165 Fontes, J.C. and Gonfiantini, R. Comportement isotopique au cours de l'évaporation de deux bassins sahariens. *Earth Planet. Sc. Lett.*, 3, 258–266, doi: 10.1016/0012-821X(67)90046-5, 1967.
- Gallart, F., Cid, N., Latron, J., Llorens, P., Bonada, N., Jeuffroy, J., Jiménez-Argudo, S.M., Vega, R.M., Solà, C., Soria, M., Bardina, M., Hernández-Casahuga, A.J., Fidalgo, A., Estrela, T., Munné and A., Prat, N. TREHS: An open-access software tool for investigating and evaluating temporary river regimes as a first step for their ecological status assessment. *Sci. Total Environ.* 2017, 607–608, 519–540, doi: 10.1016/j.scitotenv.2017.06.209, 2017.
- 170 Gat, J. R.: Oxygen and hydrogen isotopes in the hydrologic cycle, *Annu. Rev. Earth Pl. Sc.*, 24, 225–262, doi: 10.1146/annurev.earth.24.1.225, 1996.
- Gibson, J.J.: Short-term evaporation and water budget comparisons in shallow Arctic lakes using non-steady isotope mass balance. *J. Hydrol.* 264, 242–261, doi: 10.1016/S0022-1694(02)00091-4, 2002.
- 175 Gibson, J. J., Birks, S. J. and Edwards, T. W. D.: Global prediction of  $\delta_A$  and  $\delta^2\text{H}-\delta^{18}\text{O}$  evaporation slopes for lakes and soil water accounting for seasonality, *Global Biogeochem. Cycles*, 22, GB2031, doi:10.1029/2007GB002997, 2008
- Gibson, J. J., Birks, S., and Yi, Y.: Stable isotope mass balance of lakes: a contemporary perspective, *Quaternary Sci. Rev.*, 131, 316–328, doi: 10.1016/j.quascirev.2015.04.013, 2016.
- Gonfiantini, R.: Environmental isotopes in lake studies, in: *The Terrestrial Environment*, B, Handbook of Environmental Isotope Geochemistry, edited by: Fritz, P. and Fontes, J., Elsevier, Amsterdam, 113–168, doi: 10.1016/B978-0-444-42225-5.50008-5, 1986.
- 180 Hamilton, S.K., Kellogg, W.K., Bunn, S.E., Thoms, M.C. and Marshall, J.C.: Persistence of aquatic refugia between flow pulses in a dryland river system (Cooper Creek, Australia). *Limnol. Oceanogr.* 50, 743–754, doi: 10.4319/lo.2005.50.3.0743, 2005
- 185 Horita, J. and Wesolowski, D.: Liquid-Vapor Fractionation of Oxygen and Hydrogen Isotopes of Water from the Freezing to the Critical-Temperature, *Geochim. Cosmochim. Ac.*, 58, 3425–3437, doi: 10.1016/0016-7037(94)90096-5, 1994.
- Horita, J., Rozanski, K., and Cohen, S.: Isotope effects in the evaporation of water: a status report of the Craig– Gordon model, *Isotop. Environ. Health Stud.*, 44, 23–49, doi: 10.1080/10256010801887174, 2008.
- Llorens, P., Gallart, F., Cayuela, C., Roig-Planasdemunt, M., Casellas, E., Molina, A. J., Moreno de las Heras, M., Bertran, G., Sánchez-Costa, E. and Latron, J.: What have we learnt about Mediterranean catchment hydrology? 30 years observing hydrological processes in the Vallcebre research catchments, *Geographical Research Letters*, 44: 475–502, doi: 10.18172/cig.3432, 2018.
- 190 Mayr, C., Lücke, A., Stichler, W., Trimborn, P., Ercolano, B., Oliva, G., Ohlendorf, C., Soto, J., Fey, M., Haberzettl, Torsten, Janssen, S., Schäbitz, F., Schleser, G.H., Wille, M. and Zolitschka, B.: Precipitation origin and evaporation of lakes in semi-arid Patagonia (Argentina) inferred from stable isotopes ( $\delta^{18}\text{O}$ ,  $\delta^2\text{H}$ ), *J. Hydrol.*, 334(1–2), 53–63, doi: 10.1016/j.jhydrol.2006.09.025, 2007.



Merlivat, L.: Molecular diffusivities of  $\text{H}_2^{16}\text{O}$ ,  $\text{HD}^{16}\text{O}$ , and  $\text{H}_2^{18}\text{O}$  in gases, *J. Chem. Phys.*, 69, 2864–2871, <https://doi.org/10.1063/1.436884>, 1978.

200 Skrzypek, G., Mydlowski, A., Dogramaci, S., Hedley, P., Gibson, J. J., and Grierson, P. F.: Estimation of evaporative loss based on the stable isotope composition of water using Hydrocalculator. *J. Hydrol.*, 523, 781–789, doi: 10.1016/j.hydrol.2015.02.010, 2015

*Data availability.* The data are available from Pilar Llorens ([pilar.llorens@idaea.csic.es](mailto:pilar.llorens@idaea.csic.es)) upon request.

205 *Author contributions.* PL and FG designed and carried out the field experiment. SG, FG and PL did the calculations and model implementation. FG prepared the initial draft of the article. All the authors revised and accepted the final document.

*Competing interests.* The authors have the following competing interests: at least one of the (co-) authors is a member of the editorial board of Hydrology and Earth System Sciences.

210

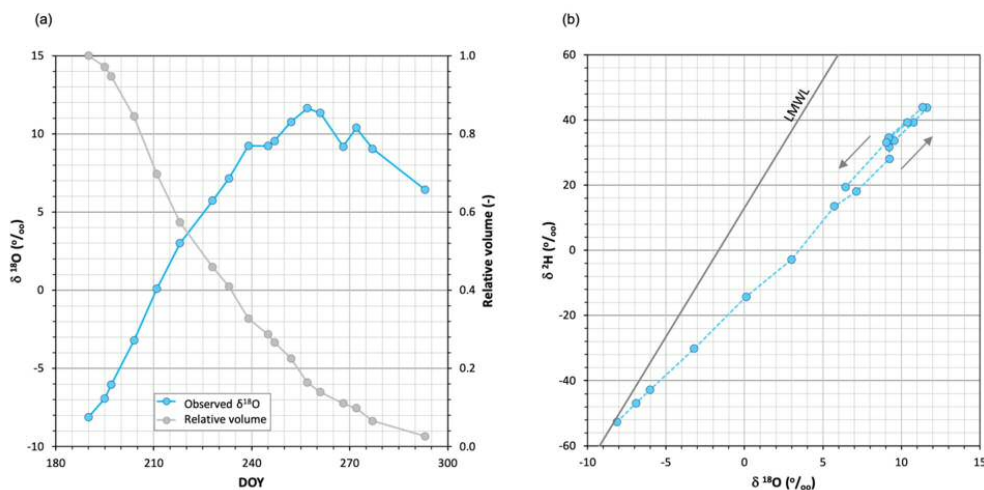
*Acknowledgements.* We are grateful to Gisel Bertran, Jérôme Latron, and both the TRivers-P project and FEHM teams for their assistance. We are also grateful to Michael Eaude for his English style improvements.

215 *Financial support.* This research was supported by the TRivers-P project (ACA210/18/00022), funded by the Catalan Water Agency (ACA), and by the Rhysotto project (PID2019-106583RB-100) funded by the Spanish Agencia Estatal de Investigación.

## Figures



220 **Figure 1:** View of steel experimental pan. The pan was partly buried in the ground and protected against precipitation by a lid of clear methacrylate installed 0.5 m above the pan surface, to allow air circulation, and against large animals drinking by a net.



225 **Figure 2:** a) Time series of  $\delta^{18}\text{O}$  concentrations of water sampled in the pan and of the relative residual volume. b) Dual plot showing the isotopic concentration of the water sampled in the pan during the studied period. The Local Meteoric Water Line (LMWL) is also indicated. Note that the depletion of heavy isotopes followed the same Local Evaporation Line as enrichment.

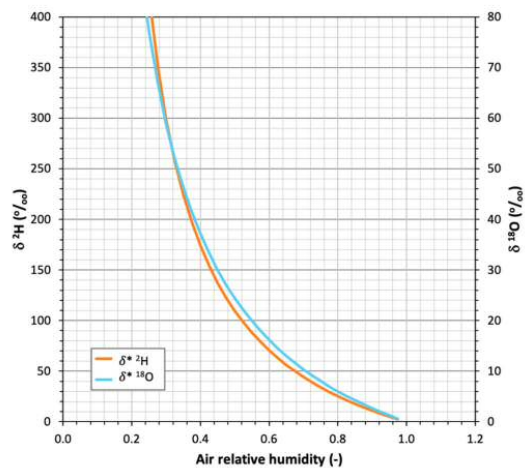
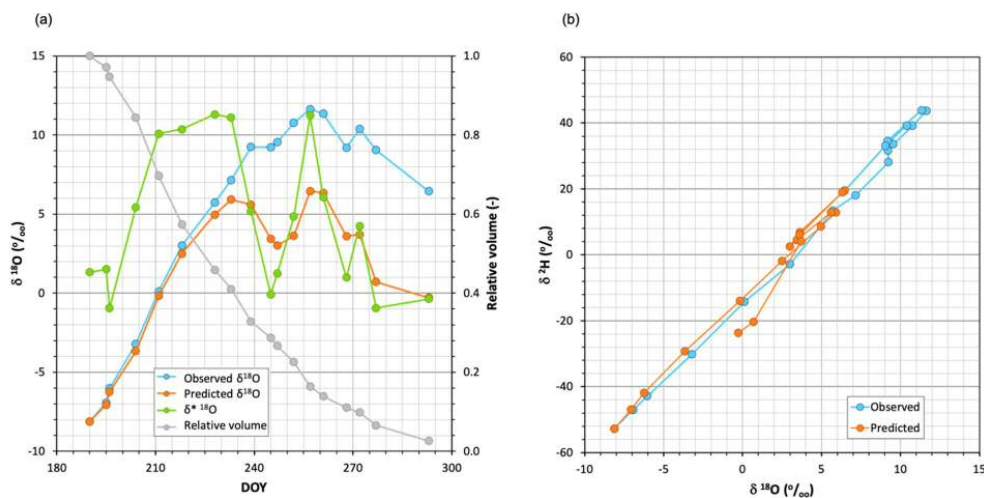
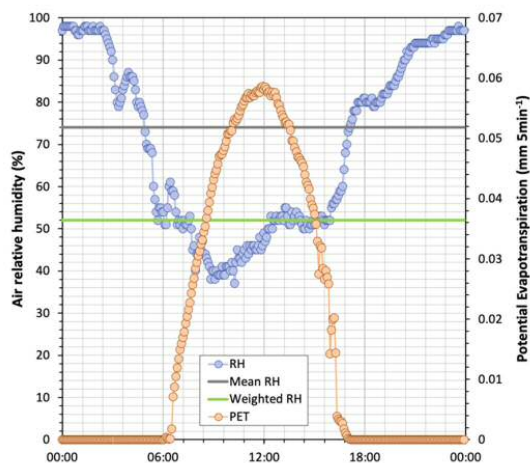


**Figure 3:** Relationship between air relative humidity and stationary isotopic compositions ( $\delta^*$ ) for  $^2\text{H}$  and  $^{18}\text{O}$  calculated using equation (2). The isotopic composition of the precipitation water is set at  $\delta=0$  for both isotopes and temperature is set at  $T=20^\circ\text{C}$ .



230 Figure 4: a) Time series of  $\delta^{18}\text{O}$  observed and simulated and  $\delta^{218}\text{O}$  when equation (1) was applied, using the weekly-averaged air temperature and relative humidity of the period studied. The relative residual volume curve is also indicated. b) Dual plot of the  $\delta^{18}\text{O}$  observed and predicted during the period studied.



235 Figure 5: Daily time series of air relative humidity and potential evaporation for 4 September, 2020 (five-minute time steps). The mean relative humidity and relative humidity weighted by evaporation flux are also shown.



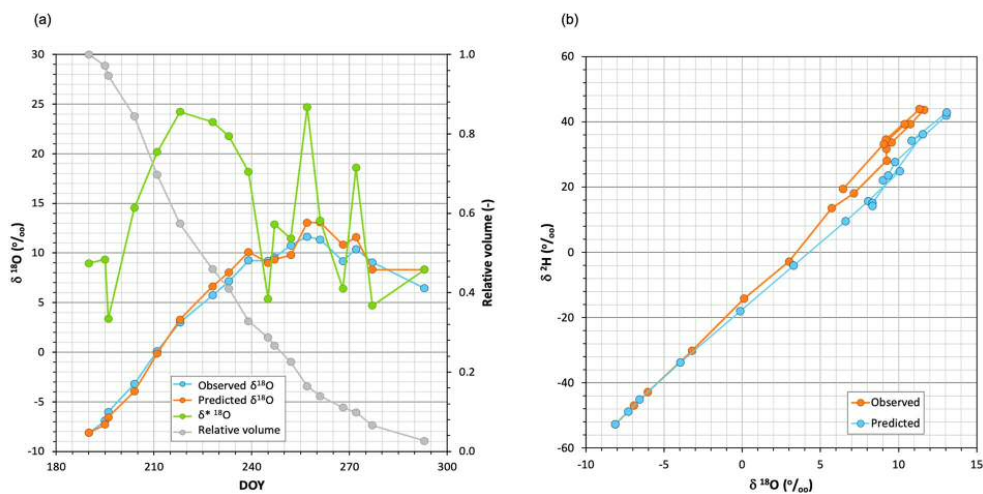


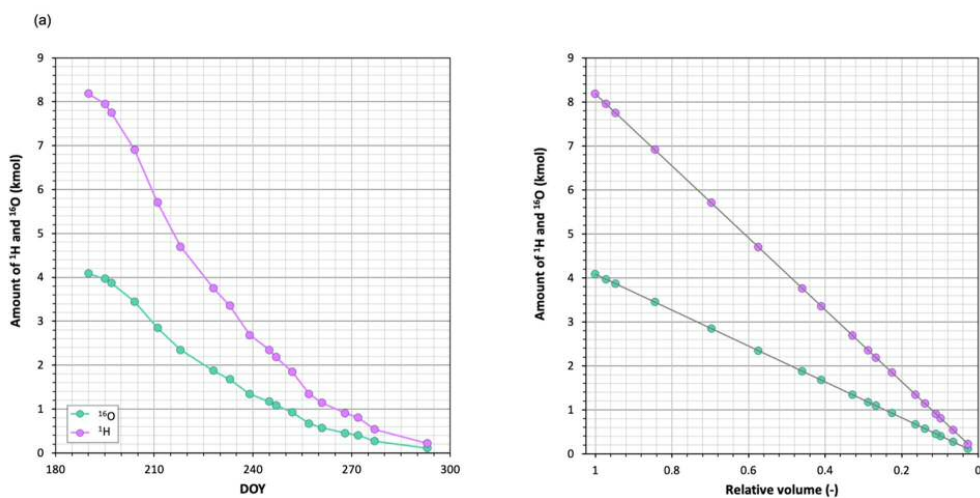
Figure 6: a) Time series of  $\delta^{18}\text{O}$  observed and simulated and  $\delta^{2}\text{H}$  when equation (1) was applied, using evaporation flux-averaged air temperature and relative humidity conditions. b) Dual plot of the  $\delta^{18}\text{O}$  observed and predicted during the period studied.

240

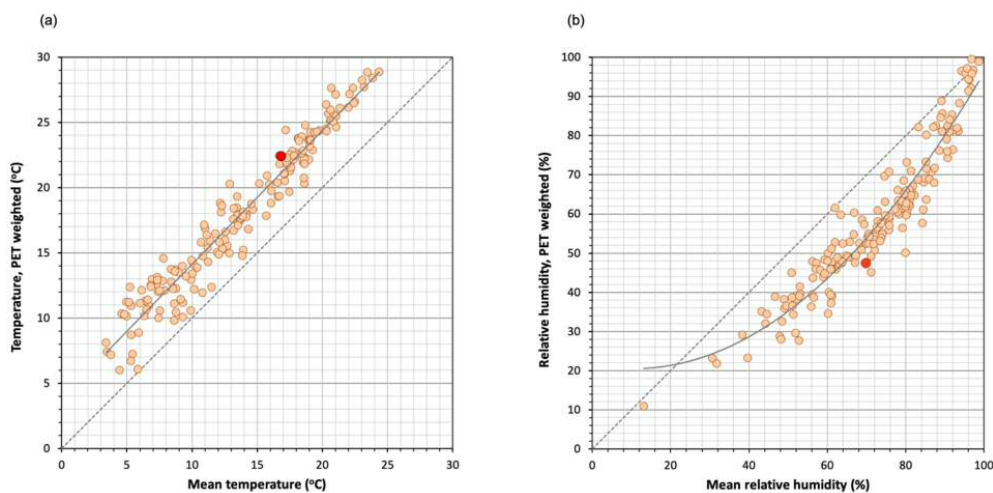


## Appendix A

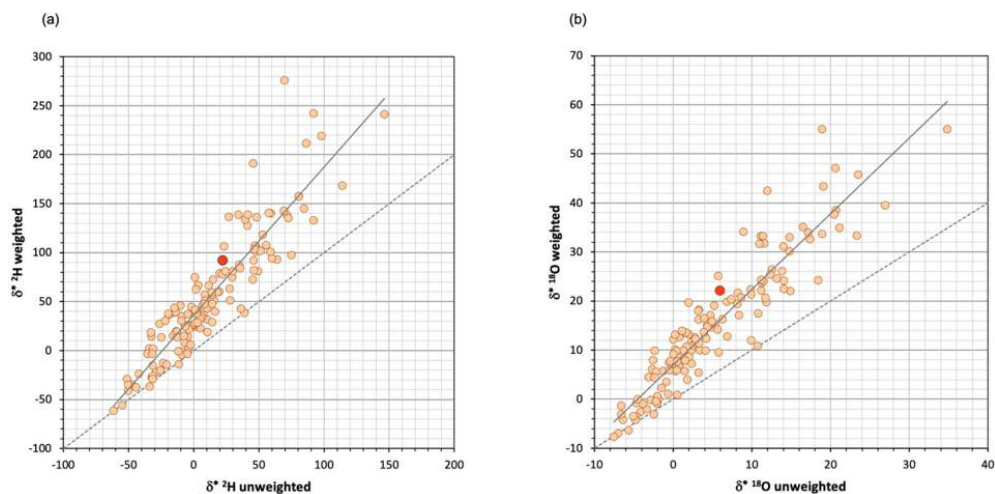
Some complementary figures included in this Appendix give further details on the experiment.



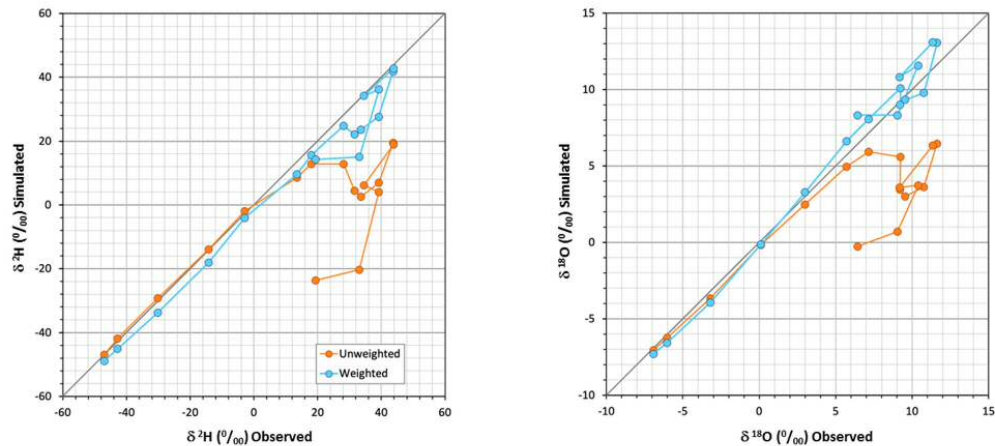
245 Figure A1: Amount of light isotopes in the water during the experiment, a) for the date and b) for the relative residual volume. Evaporation rates always exceeded condensation ones, including during the late periods of heavy isotope depletion.



250 Figure A2: Comparison of the differences in daily a) temperature and b) relative humidity when 5-minute readings were time-averaged or weighted with potential evapotranspiration. Temperatures became similarly higher when flux-averaged, regardless of their magnitude. In a different way, relative humidity was habitually lower when flux-averaged, but did not change when it was very high or very low. The red dots represent the conditions on the date shown in Figure 5. The dashed line shows the 1:1 relationship.



255 **Figure A3:** Comparison of the differences in daily a) temperature and b) relative humidity when 5-minute readings were time-averaged or weighted with potential evapotranspiration. Low  $\delta^*$  values show the least differences because these correspond to days with high relative humidity, as shown in Figure 3. The red dots represent the conditions on the date shown in Figure 5. The dashed line shows the 1:1 relationship.



260 **Figure A4:** Simulated *versus* observed heavy isotope concentrations when air temperature and relative humidity are time-averaged or weighted with potential evapotranspiration. When using flux-weighting, mean absolute errors decreased by a quotient of 4, from 19.31 and 3.78‰ for  $\delta^2\text{H}$  and  $\delta^{18}\text{O}$ , respectively, to 4.88 and 0.87‰.